Nuclear Inst. and Methods in Physics Research, A 887 (2018) 144–149

Contents lists available at ScienceDirect

Nuclear Inst. and Methods in Physics Research, A

journal homepage: www.elsevier.com/locate/nima

Technical notes

Characterization of silicon photomultipliers and validation of the electrical model

Peng Peng [a,b,*], Yi Qiang [a], Steve Ross [a], Kent Burr [a]

[a] Toshiba Medical Research Institute USA, 706 N Deerpath Drive, Vernon Hills, IL 60061, USA
[b] Department of Biomedical Engineering, University of California-Davis, One Shields Avenue, Davis, CA 95616, USA

ARTICLE INFO

Keywords:
SiPM
PET
Characterization

ABSTRACT

This paper introduces a systematic way to measure most features of the silicon photomultipliers (SiPM). We implement an efficient two-laser procedure to measure the recovery time. Avalanche probability was found to play an important role in explaining the right behavior of the SiPM recovery process. Also, we demonstrate how equivalent circuit parameters measured by optical tests can be used in SPICE modeling to predict details of the time constants relevant to the pulse shape. The SiPM properties measured include breakdown voltage, gain, diode capacitor, quench resistor, quench capacitor, dark count rate, photodetection efficiency, cross-talk and after-pulsing probability, and recovery time. We apply these techniques on the SiPMs from two companies: Hamamatsu and SensL.

1. Introduction

Silicon photomultipliers(SiPMs) have become excellent candidates to replace photomultiplier tubes (PMT) in next-generation positron emission tomography (PET) and single photon emission computed tomography (SPECT) medical scanners [1–5]. Compared with PMTs, SiPMs have the following advantages: high quantum efficiency, low operation voltage, insensitivity to magnetic field, mechanical robustness, compactness, uniform gain, and high degree of scalability. Relative drawbacks have been their high dark count rate, cross-talk, after-pulsing, and cost. However, recent technological advances have led to the development of the low dark count rate, and low cross-talk and after-pulsing SiPMs [6–8]. In order to optimize the design for PET or SPECT applications it is essential to have a good understanding of the properties and a reasonable electrical model for the SiPM.

In this paper, we have studied the following SiPM properties: breakdown voltage, avalanche gain, diode capacitance, quench resistance and capacitance, dark count rate (DCR), photodetection efficiency (PDE), cross-talk and after-pulsing probability, and recovery time. Two SiPMs were used in this study: Hamamatsu MPPC (S12642-0404PB-50X), and SensL C-Series (microFC 60035). The Hamamatsu MPPC is a 4 by 4 SiPM array, with pixel dimension 3 mm by 3 mm. There are 3600 microcells in each pixel with a cell pitch of 50 μm. The SensL SiPM is a 6 mm by 6 mm single pixel, with 18 980 microcells in the pixel, and each microcell has an active area of 35 μm by 35 μm. Compared with previous studies of the characterization of the SiPM [9], a new setup and a new analysis method were implemented in this paper, which enable us to extract the properties of the SiPM in three tests with the same setup.

2. Materials and methods

2.1. Experimental setups

Three tests were conducted in this study: low intensity light test, forward bias voltage test, and recovery time test. All three tests used laser (Photek LPG-405) as the light source for the SiPM (Fig. 1). The low intensity light and forward bias voltage tests used one laser, the recovery time test used two lasers. In the low intensity light test, SiPM signals went through a voltage feedback amplifier (OPA4820) with a gain of 20 and were then recorded with the digitizer (CAEN DT5742). In the forward bias voltage and recovery time test, SiPM signals were recorded by the oscilloscope (Agilent Infiniium DSA80000B) directly. The incident photon intensity was calibrated using Thorlabs FDS100 photodiode with a relative uncertainty less than 10%.

2.2. Low intensity light test

In the first test, a low intensity light was used to measure the single photoelectron spectrum. Fig. 2 shows the spectrum for the Hamamatsu

* Corresponding author at: Department of Biomedical Engineering, University of California-Davis, One Shields Avenue, Davis, CA 95616, USA.
E-mail address: pppeng@ucdavis.edu (P. Peng).

https://doi.org/10.1016/j.nima.2018.01.059
Received 20 December 2017; Received in revised form 11 January 2018; Accepted 16 January 2018
0168-9002/

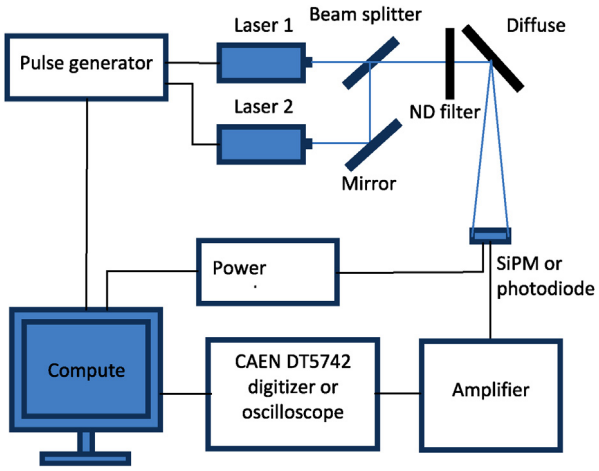

Fig. 1. Schematic layout of the experimental setup. The light source was the Photek LPG-405 pulse laser producing 115 ps, 405 nm light pulses. The two lasers were set to have approximately the same intensities at the location of the photodetector. The photodetector was a photodiode or a SiPM. The data acquisition system used a digitizer or an oscilloscope for different tests. LabView programs were built to control all the devices.

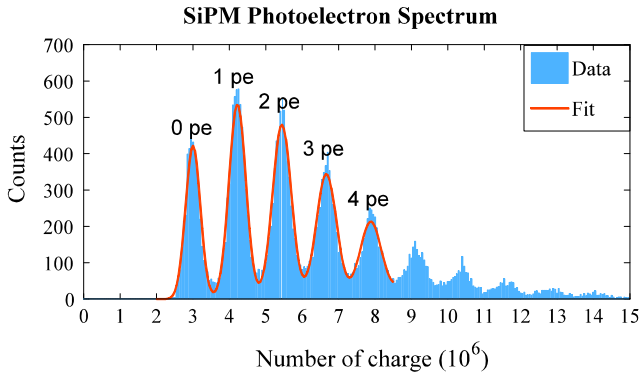

Fig. 2. Photoelectron spectrum for Hamamatsu MPPC measured at bias voltage of $V_{\text{bias}} = 66$ V, and temperature $T = 24.2$ °C. If there were no cross-talk or after-pulsing then the signal heights from the few photons would fit a single Poisson distribution, two being used to account for these effects. The fitting function gives the following information: gain (G), average fired microcells (μ), cross-talk and after-pulsing probability (δ)

SiPM with bias voltage $V_{\text{bias}} = 66$ V at room temperature (24.2 °C). We used a convolution of a discrete distribution function and a Gaussian function to fit the spectrum [10]:

$$A(x) = A_0 \cdot P(n|\mu, \Delta\mu) \otimes Gaus\left(x|n \cdot G + ped, \sigma_n\right) \tag{1}$$

$$P(n|\mu, \Delta\mu) = \sum_{i+j=n} \frac{\mu^i e^{-\mu}}{i!} \cdot \frac{(i \cdot \Delta\mu)^j e^{-(i\cdot\Delta\mu)}}{j!}. \tag{2}$$

The discrete function $P(n|\mu, \Delta\mu)$, Eq. (2), represents the distribution of total number of fired microcells, which contains two Poisson distributions: one is for the primary fired microcells with an average number of μ, the other is for the microcells fired in the process of cross-talk and after-pulsing with an average number of $\Delta\mu$ per primary fired microcell. The Gaussian function represents the distribution of charge for each n. It has a mean value of $n \cdot G + ped$, where G is the SiPM gain and ped is the pedestal value. The width of the Gaussian function contains three parameters: n, σ_{ped} (the width of the pedestal) and σ_{sig} (the width of a single microcell signal), as

$$\sigma_n = \sqrt{\sigma_{ped}^2 + n \cdot \sigma_{sig}^2}. \tag{3}$$

Our fit to this spectrum gives the SiPM properties: gain, average fired microcells, and cross-talk combined with after-pulsing probability, as listed in Tables 1 and 2. The tests were conducted with five different bias voltages and three different light intensities for both the Hamamatsu and SensL SiPMs.

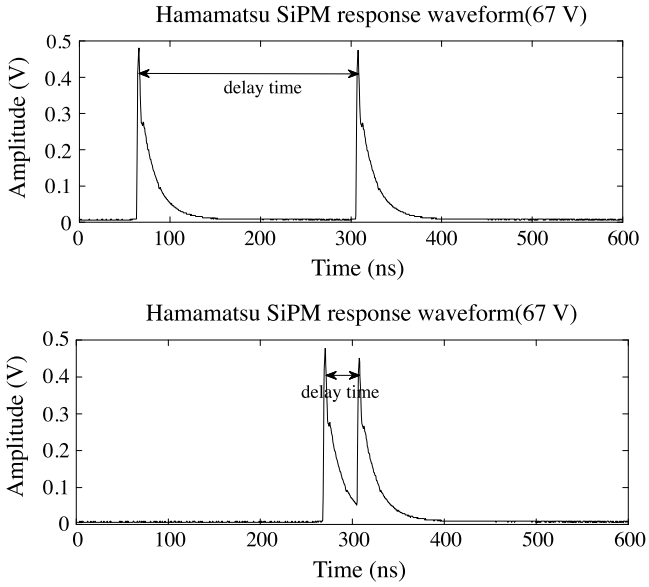

Fig. 3. SiPM response waveform of two sequential laser pulses with different delay time for Hamamatsu MPPC.

2.3. Forward bias voltage test

In the second test, the resistance of the SiPM's quench resistor was measured by applying a forward bias voltage to the SiPM. The value of quench resistor can be calculated as:

$$R_q = \left(\frac{1}{k} - R_s\right) \cdot N, \tag{4}$$

where k is the slope from the linear fit of the IV curve, R_s is the external resistor connected in series with the SiPM, and N is the number of microcells in one SiPM pixel.

2.4. Recovery time test

In the recovery time test, both pulsed lasers shown in Fig. 1 were triggered by the pulse generator. Each laser spot was sized larger than the SiPM's active area to make sure the light field was uniform on the SiPM. The second laser was triggered relative to the first with an adjustable positive or negative delay t_{delay}. Fig. 3 shows the signals from the SiPM with two different values for t_{delay}. We observed that if the time between the two pulses were close, the magnitude of the waveform for the second pulse was smaller, due to the recovery process of the SiPM. The integral of the pulses in Fig. 3 was proportional to the total charge induced in the SiPM by the two laser pulses. Fig. 4 shows its dependence on the delay time.

A fitting function, Eq. (5), is used to fit the plot in Fig. 4:

$$\overline{Q_{total}} = \overline{N_1} C V_{over} + \overline{N_2} \cdot CV(t) \cdot \eta(t). \tag{5}$$

The first term represents the average charge released without going through the recovery process. The second term represents the average charge released during the recovery process. C is the microcell capacitance, $\overline{N_1}$ and $\overline{N_2}$ are the average numbers of microcells that correspond to the two terms. There are two components that affect the process of the SiPM's recovery. The first component is the voltage recovery as shown in Eq. (6), where τ is the cell recovery time constant. The second component is the relative time dependent avalanche probability